INFECTION AND IMMUNITY, Feb. 2010, p. 618–628 Vol. 78, No. 2
0019-9567/10/$12.00 doi:10.1128/IAI.00647-09

Differential Patterns of Liver Proteins in Experimental Murine Hepatosplenic Schistosomiasis▽†

B. Manivannan,[1] P. Rawson,[1] T. W. Jordan,[1] W. E. Secor,[2] and A. C. La Flamme[1]*

Centre for Biodiscovery and School of Biological Sciences, Victoria University of Wellington, Wellington, New Zealand,[1] and Centers for Disease Control and Prevention, Atlanta, Georgia[2]

Received 8 June 2009/Returned for modification 17 July 2009/Accepted 13 November 2009

***Schistosoma mansoni* eggs produced by adult worms in the mesenteric vasculature become trapped in the liver, where they induce granulomatous lesions and strong immune responses. Infected individuals suffer from intestinal schistosomiasis (INT) in 90% of cases, whereas the remaining 10% present with severe hepatosplenic schistosomiasis (HS). The CBA/J mouse model mimics human disease, with 20% of infected mice developing hypersplenomegaly syndrome (HSS) that resembles HS and 80% developing moderate splenomegaly syndrome (MSS) similar to INT. We studied differential patterns of protein expression in livers of 20-week-infected CBA/J mice with MSS or HSS to understand the molecular changes that underlie these two disease forms. Using differential in-gel electrophoresis to identify differentially expressed protein spots, we found 80 protein spots significantly changed with infection and 35 changes specific to severe disease. In particular, the abundances of prohibitin 2, transferrin isoforms, and major urinary protein isoforms were significantly altered in HSS mice. Furthermore, annexin 5, glutathione *S*-transferase pi class, and *S. mansoni* phosphoenolpyruvate carboxykinase expression levels changed significantly with schistosome infection. Additionally, levels of major urinary protein decreased and levels of transferrin increased significantly in the sera of HSS mice compared to levels in sera of MSS or control mice, and these differences correlated to the degree of splenomegaly. These findings indicate that the liver protein abundances differ between MSS and HSS mice and may be used for the development of diagnostic markers for the early detection of hepatosplenic schistosomiasis.**

Schistosomiasis affects 200 million people worldwide (13), and *Schistosoma mansoni*-associated hepatomegaly is estimated to affect 8.5 million people (62). From animal studies, it is estimated that the acute phase of infection for schistosomiasis occurs roughly 5 to 6 weeks after infection, when the parasitic eggs are swept into the liver microvasculature and induce granulomatous lesions. The chronic phase begins more than 12 weeks postinfection, with periportal liver fibrosis and extreme splenomegaly. In 90% of infected individuals, the egg-associated inflammation recedes, resulting in intestinal schistosomiasis (INT). In contrast, 10% of infected individuals present with severe hepatic and periportal fibrosis, portal hypertension, and portal-systemic venous shunts due to hepatic granulomas; these contribute to life-threatening hepatosplenic schistosomiasis (HS) (27). Granulomas play an important role in the development of the severe pathology of schistosomiasis (56). Previous studies have shown that the development of schistosomiasis causes liver dysfunction by altering metabolic processes through the upregulation or downregulation of enzymes (25, 67). Despite successful control measures for schistosomiasis in many countries, population growth and movement (13) and risk of reinfection (38) have played major roles in the transmission and spread of schistosomiasis to new areas.

Our research focuses on an understanding of the protein patterns associated with the two distinct pathological forms of schistosomiasis. We used the CBA/J mouse model, as it reproduces human disease forms, with 20% of CBA/J mice developing hypersplenomegaly syndrome (HSS), which resembles HS, and 80% of the mice developing moderate splenomegaly syndrome (MSS), which is similar to INT (27). We have used two-dimensional differential in-gel electrophoresis (2D-DIGE) wherein protein samples are prelabeled with CyDyes before two-dimensional electrophoresis (2DE) for differential analysis, enabling the accurate tracking of qualitative and quantitative differences between MSS and HSS samples. Matrix-assisted laser desorption ionization (MALDI)–time of flight (TOF) mass spectrometry was used to identify protein spots that changed during the development of MSS and HSS. We believe that identifying disease-specific proteins may contribute to the early detection of and treatment strategies for hepatosplenic schistosomiasis.

MATERIALS AND METHODS

Mouse model and liver sample collection. Male CBA/J mice were obtained from the Jackson Laboratory and were maintained at the American Association for Accreditation of Laboratory Animal Care, Centers for Disease Control and Prevention, in accordance with institutional guidelines and federal regulations. Mice were infected by the subcutaneous injection of 45 cercariae of a Puerto Rican strain of *S. mansoni* that had been maintained in *Biomphalaria glabrata* snails. At 20 weeks of infection, animals were sacrificed and classified as having MSS or HSS based on percent spleen body weight and gross pathological appearance (27). Liver and serum samples were collected from the three groups (uninfected age-matched controls, MSS, and HSS; $n = 5$ per group) and snap-frozen at −80°C. A similar but different set of liver samples was collected from uninfected age-matched control, MSS, and HSS groups as described above along with liver samples from 12-week-infected CBA/J mice ($n = 10$) and stored at −80°C. All the samples were collected within the same time period to avoid bias

* Corresponding author. Mailing address: School of Biological Sciences, Victoria University of Wellington, P.O. Box 600, Wellington, New Zealand. Phone: 64-4-463-6093. Fax: 64-4-463-5331. E-mail: anne.laflamme@vuw.ac.nz.

† Supplemental material for this article may be found at http://iai.asm.org/.

▽ Published ahead of print on 23 November 2009.

due to collection time. The Victoria University of Wellington Animal Ethics Committee approved all experiments.

Extraction of protein from liver tissue. For each liver sample, approximately 10 mg of tissues was homogenized in 100 μl standard lysis buffer containing 30 mM Tris-HCl (Sigma-Aldrich, St. Louis, MO), 2 M thiourea (Merck, Darmstadt, Germany), 7 M urea (Merck), and 4% (wt/vol) CHAPS {3-[(3-cholamidopropyl)-dimethylammonio]-1-propanesulfonate} (Sigma-Aldrich). Homogenates were vortexed for 10 min and centrifuged at 13,000 rpm for 10 min. The protein concentration was determined by using a 2D-Quant kit (GE Healthcare, Uppsala, Sweden) (7). Lysates were stored at −20°C until further use.

Differential in-gel electrophoresis (DIGE) with CyDyes. Liver lysates and sera were thawed, vortexed, and centrifuged before labeling, and the pH was adjusted to 8.5 by the addition of 1.5 M Tris-HCl (pH 8.5). The Minimal CyDye kit (GE Healthcare) was used to label the liver lysates according to the manufacturer's recommended protocol. The internal standard, a pool of all 15 lysates, was labeled using Cy2; individual samples were labeled with Cy3 and Cy5. Ten micrograms of protein was labeled with 80 pmol of amine-reactive CyDyes reconstituted in anhydrous dimethylformamide (Sigma-Aldrich) for 30 min at 4°C in the dark. The reaction was quenched by the addition of 1 μl 10 mM lysine to the mixture (7). Labeled samples were combined for electrophoresis as indicated in Table S1 in the supplemental material.

Two-dimensional gel electrophoresis. Seven-centimeter Immobiline immobilized pH gradient (IPG) DryStrips (pH 4 to 7) were placed in contact with the labeled protein sample diluted to 125 μl with rehydration buffer containing 2 M thiourea, 7 M urea, 2% IPG buffer (pH 3 to 10; GE Healthcare), 2% dithiothreitol (DTT), 4% (wt/vol) CHAPS, and 0.5% bromophenol blue. The strips were subjected to first-dimension separation by using an IPGphor system (GE Healthcare) with the following protocol: temperature of 20°C; current of 50 μA per strip; and 300 V (step) for 30 min, 1,000 V (gradient) for 30 min, 5,000 V (gradient) for 85 min, and 5,000 V (step) for 25 min. The 7-cm IPG strips (pH 6 to 11; GE Healthcare) were subjected to overnight rehydration without the CyDye-labeled sample by using 125 μl rehydration buffer containing 2 M thiourea, 4 M urea, 1% IPG buffer (pH 6 to 11; GE Healthcare), 2% (wt/vol) CHAPS, 10% isopropanol, 2.5% DTT, 5% glycerol, and 0.5% bromophenol blue. Labeled samples were diluted to 100 μl with rehydration buffer and incubated overnight in the dark at room temperature. A Multiphor II system (GE Healthcare) was used to focus IPG (pH 6 to 11) strips by using the following protocol: temperature of 20°C; current of 2 mA per strip; and 200 V (step) for 1 min, 3,500 V (gradient) for 90 min, and 3,500 V (gradient) for 64 min. Samples were loaded by cup loading at the anodic end. The focused strips were equilibrated at room temperature for 10 min in equilibration buffer (50 mM Tris [pH 8.8], 6 M urea, 30% glycerol, 2% SDS, 0.5% bromophenol blue) with 1% DTT, followed by an equilibration at room temperature for 10 min in equilibration buffer with 2.5% (wt/vol) iodoacetamide. The equilibrated strips were electrophoresed on NuPAGE Novex 4 to 12% Bis-Tris Zoom gels and IPG Well (1.0 mm) (Invitrogen, Carlsbad, CA) using NuPAGE MOPS (morpholinepropanesulfonic acid) SDS running buffer with the addition of 0.5 ml NuPAGE antioxidant (Invitrogen) in the inner chamber (7). The pH 3 to 10 strips for serum DIGE were electrophoresed by using the same procedure as that described above for the pH 4 to 7 strips.

Scanning of DIGE-labeled images. Gels were scanned by using a Fuji film FLA-5100 apparatus (Fuji Photo Film Co., Tokyo, Japan). The Cy2, Cy3, and Cy5 images were scanned sequentially. The filter specifications for Cy2, Cy3, and Cy5 images were described previously (7).

Image analysis. DIGE gels were analyzed for differentially expressed proteins using DeCyder 2-D 6.5 software (GE Healthcare). The internal standard assisted in linking protein spots in the gel, giving an accurate quantitation and minimizing the effects of variation between gels. The standard was included for all gels, and each gel was matched to the standard. The biological variation analysis (BVA) module was used for matching multiple gels, comparing protein spots, and calculating statistics for differences in protein spot abundance. The spot detection limit was set to 2,500. The difference in protein spots between gels is expressed by using the average volume ratio among the three groups, with "+" indicating the increase in the average volume ratio and "−" indicating the decrease in the average volume ratio (Table 1). The false discovery rate (FDR) is a statistical method to interpret the proportion of false-positive results among those proteins that are thought to be significantly changed. Due to the high dimensionality of the data, the FDR feature was applied as a multiple-test correction to minimize the false-positive discovery of protein spots and keep the overall error rate low. The data were analyzed according to the guidelines for a target power of 0.8 (i.e., a 2-fold change in the average volume ratio can be accepted using four replicates with a one-way analysis of variance [1-ANOVA] value of ≤0.01) (31, 32). Multivariate analysis was performed by using the DeCyder-Extended data analysis module with the principle-component analysis (PCA) and hierarchical cluster analysis (HCA) features. PCA and HCA reduced the multidimensionality of the protein spot data across gel images. Individual spot volumes extracted from the DeCyder software were compared by use of GraphPad Prism v 4 software. Protein spot Gene Ontology functional data were plotted by using SPSS 16.0.1 software.

Spot picking and enzymatic digestion. The preparative gels (75 μg protein per gel) for liver lysates and sera were fixed, prestained, and stained as described previously (25). The gels were scanned by using a Molecular Dynamics (Sunnyvale, CA) Personal Densitometer SI scanner. Spots were excised from the preparative gels by using a 1.5-mm Spot Picker Plus apparatus (The Gel Company, San Francisco, CA) and transferred into v-bottom-shaped 96-well polypropylene plates (Greiner Bio-One, Germany). An Ettan digester (GE Healthcare) was used for destaining and to perform in-gel digestion of gel plugs by using the following protocol. The gels plugs were washed four times for 30 min with 100 μl 50 mM NH_4HCO_3 (Sigma-Aldrich) in 50% methanol (Merck) and dried at room temperature for 60 min. Ten microliters of trypsin (0.05 μg/10 μl in 20 mM NH_4HCO_3) (trypsin-modified sequencing grade; Roche Diagnostics, Germany) was added to each well, and digestion was carried out for 6 h at room temperature. The tryptic digests were transferred onto a fresh plate, and the gel plugs were washed with 10 μl 0.1% trifluoroacetic acid (TFA) (Sigma-Aldrich) in 50% acetonitrile (Merck) for 20 min two times each. The digestion and wash solutions were collected and combined. The tryptic peptides were dried overnight completely in a laminar flow hood.

Protein identification by mass spectrometry. The dried tryptic digests were resuspended in 1 μl of 10 mg/ml α-cyano-4-hydroxycinnamic acid (CHCA; Sigma-Aldrich) solution prepared in a 50% (vol/vol) solution of acetonitrile and 0.25% TFA and spotted onto a MALDI plate and air dried prior to mass spectrometry. All tryptic digests were analyzed by MALDI-TOF (Voyager-DE Pro MALDI-TOF mass spectrometer; Applied Biosystems, Foster City, CA). The spectra were collected over the range *m*/*z* 800 to 3,500. External calibration was performed by using calibration mixture 2 of the Sequazyme peptide mass standard kit (Applied Biosystems), containing angiotensin I (*m*/*z* 1,297.51), fragments of the adrenocorticotropic hormone 1-17 (*m*/*z* 2,094.46), and 18-39 (*m*/*z* 2,466.72). Internal calibration was performed by using monoisotopic trypsin peaks (*m*/*z* = 805.41 and 2,163.05). Spectra were processed by using Data Explorer software (v 5.1; Applied Biosystems) to generate monoisotopic peptide masses, which were used to identify proteins using Mascot Server, MatrixScience, v 2.1.03, against the complete NCBInr and schistosome database (updated 27 March 2007). Complete cysteine modification by iodoacetamide, methionine partial modification by oxidation, 50 ppm peptide tolerance, and one missed trypsin cleavage were included as search parameters. Criteria for a match included the number of peptides matched, sequence coverage, and the difference in probability between the first and second matches (7).

Western blots. Liver lysate proteins separated by one-dimensional electrophoresis on a 1.0-mm 12-well NuPAGE Bis-Tris gel (Invitrogen) were transblotted onto Hybond-LFP, a low-fluorescent, hydrophobic polyvinylidene difluoride (PVDF) membrane (GE Healthcare). The proteins were blotted at 25 V for 2.5 h and blocked for 1 h at room temperature by using 5% nonfat dry milk in Tris-buffered saline–Tween (TBST) (pH 7.4) for phosphoenolpyruvate carboxykinase (PEPCK) and 1% casein (Merck) in TBST for major urinary protein (MUP) and transferrin. The membranes were washed three times for 5 min with TBST and probed with primary polyclonal antibodies (PEPCK rabbit polyclonal antibody, MUP goat polyclonal antibody, and transferrin goat polyclonal antibody; Santa Cruz Biotechnology, Inc., Santa Cruz, CA) at a 1:600 dilution overnight at 4°C, followed by three washes for 5 min with TBST. This was followed by 2 h of incubation with secondary Cy5-labeled anti-rabbit and anti-goat antibodies, respectively (Jackson ImmunoResearch Laboratories, West Grove, PA) at a 1:2,000 dilution at room temperature. Mouse anti-actin monoclonal antibody (Chemicon International, Inc., Millipore, CA) was used as a loading control with Cy3-labeled anti-mouse antibody (Jackson ImmunoResearch Laboratories). Protein bands were visualized by using a Fujifilm FLA-5100 scanner (Fuji Photo Film Co.). ImageQuant 5.2v (GE Healthcare) software was used to analyze protein band volumes. Sera (10 μg protein/well, diluted 1:50 with phosphate-buffered saline [pH 7.4]) were treated similarly to liver lysates and probed for mouse transferrin by Western blotting.

RESULTS AND DISCUSSION

All of the 20-week *S. mansoni*-infected CBA/J mice had enlarged, granulomatous livers and were classified as being MSS or HSS by the percent spleen-to-body weight ratio

TABLE 1. Identified protein spot comparisons between study groups

Spot	Protein[c]	AVR[a]			gi no.	pI	Molecular mass (kDa)	Function[b]	Reference(s)
		H/C	M/C	H/M					
1	Actin	+2.12	+1.81	+1.17	809561	5.8	39.45	STR	25
2	Actin	+2.39	+2.04	+1.17	49868	5.8	39.45	STR	25
3	Albumin	+3.26	+1.88	+1.73	19353306	5.8	70.73	APP	25
4	Albumin	+2.84	+1.71	+1.66	33859506	5.8	70.73	APP	25
5	Albumin	+2.83	+1.73	+1.63	19353306	5.8	70.73	APP	25
6	Albumin	−2.13	−1.51	−1.41	26341396	5.5	67.04	APP	25
7	Aldehyde dehydrogenase 9	+2.87	+1.90	+1.51	9910128	6.6	54.47	ROX	17, 64
8	Annexin 5	+4.52	+2.17	+2.08	6753060	4.8	35.78	SIG	43
9	ATPS	−2.05	−1.88	−1.09	23272966	5.2	56.65	EGM	11, 25
10	ATPS	−2.13	−1.72	−1.24	23272966	5.2	56.65	EGM	11, 25
11	Betaine homocysteine methyltransferase 2	+3.80	+2.54	+1.50	62533211	6.0	40.28	MYL	20, 59
12	Brain and reproductive organ-expressed protein	+3.04	+2.08	+1.46	38173925	5.7	43.95	APO	12, 36
13	Carbamoyl phosphate synthase	−2.60	−1.87	−1.39	73918911	6.5	165.8	EGM	25, 60
14	Chaperonin-containing TCP-1 theta subunit	−2.85	−1.78	−1.60	5295992	5.4	60.06	PRF	1, 25
15	Collagen 6a1	+17.8	+12.2	+1.45	12805443	5.8	44.76	STR	19, 25
16	Collagen 6a1	+47.8	+32.3	+1.48	12805443	5.8	44.76	STR	19, 25
17	Collagen 6a1	+55.8	+36.2	+1.54	12805443	5.8	44.76	STR	19, 25
18	Collagen 6a1	+47.8	+31.9	+1.50	12805443	5.8	44.76	STR	19, 25
19	Collagen 6a1	+34.7	+24.2	+1.43	12805443	5.8	44.76	STR	19, 25
20	Collagen 6a1	+21.0	+15.5	+1.36	12805443	5.8	44.76	STR	19, 25
21	Collagen 6a1	+10.2	+7.81	+1.30	12805443	5.8	44.76	STR	19, 25
22	Collagen 6a1	+5.38	+4.94	+1.09	12805443	5.8	44.76	STR	19, 25
23	Collagen XIV	+5.13	+2.40	+2.13	30420885	5.0	194.3	STR	19, 25
24	Collagen XIV	+4.27	+2.78	+1.54	30420885	5.0	194.3	STR	19, 25
25	Collagen XIV	+7.13	+3.61	+1.97	30420885	5.0	194.3	STR	19, 25
26	DMDH	−2.04	−1.71	−1.20	59808083	7.8	97.44	CHO	25
27	DMDH	−2.21	−1.74	−1.27	59808083	7.8	97.44	CHO	25
28	DMDH	−2.34	−1.76	−1.33	59808083	7.8	97.44	CHO	25
29	EH	−2.46	−1.78	−1.38	15929294	5.9	63.07	XBM	44
30	EH	−2.41	−2.03	−1.19	15929294	5.9	63.07	XBM	44
31	EH	−2.82	−1.85	−1.52	15929294	5.9	63.10	XBM	44
32	10-FTHFDH	−2.52	−1.49	−1.69	20380027	5.6	99.55	MYL	33, 64
33	10-FTHFDH	−2.56	−1.43	−1.79	20380027	5.6	99.55	MYL	33, 64
34	10-FTHFDH	−2.28	−1.54	−1.48	23271467	5.6	99.55	MYL	33, 64
35	10-FTHFDH	−2.36	−1.51	−1.56	20380027	5.6	99.55	MYL	33, 64
36	10-FTHFDH	−2.47	−1.70	−1.46	23271467	5.6	99.55	MYL	33, 64
37	Glucosidase II β	+3.53	+2.47	+1.43	57013837	4.4	59.74	PRF	2, 49
38	Glucosidase II β	+2.47	+2.13	+1.16	57013837	4.4	59.74	PRF	2, 49
39	Group-specific component	+2.89	+1.81	+1.60	51172612	5.4	55.18	APP	40, 55
40	Keratin D	+2.43	+1.52	+1.60	293682	5.3	47.47	STR	9, 53
41	Lymphocyte cytosolic protein 1 (plastin 2)	+4.17	+3.06	+1.36	26326929	5.2	70.77	PRF	57
42	Plastin 2	+3.24	+2.45	+1.32	26326929	5.2	70.77	PRF	57
43	MUP	−8.11	−1.69	−4.80	53271	4.8	17.71	PHE	18
44	MUP	−7.54	−1.50	−5.02	12851568	4.8	17.71	PHE	18
45	MUP	−10.3	−2.61	−3.96	13276755	4.8	17.71	PHE	18
46	MUP	−5.56	−2.35	−2.37	494384	4.8	17.71	PHE	18
47	MUP	−3.51	−1.50	−2.34	38488789	4.8	21.73	PHE	18
48	Myosin light polypeptide 6	−2.15	−1.68	−1.28	33620739	4.6	17.09	STR	66
49	NADH dehydrogenase (ubiquinone) Fe-S protein 1	−2.12	−1.75	−1.21	21704020	5.5	80.76	EGM	8
50	Protein disulfide-isomerase A3, Erp57	+3.17	+1.94	+1.63	26353794	5.8	57.12	ROX	25, 54
51	Pyruvate carboxylase	−3.44	−2.17	−1.58	26346581	6.1	103.8	EGM	24, 25

Continued on following page

TABLE 1—*Continued*

Spot	Protein[c]	AVR[a]			gi no.	pI	Molecular mass (kDa)	Function[b]	Reference(s)
		H/C	M/C	H/M					
52	Pyruvate carboxylase	−2.35	−1.72	−1.36	26346581	6.1	103.8	EGM	24, 25
53	Retinol binding protein type I	+2.73	+1.91	+1.43	21730472	5.1	15.86	APP	61
54	RNase/angiogenesis inhibitor	+2.15	+2.16	−1.00	14577933	4.6	51.21	IMM	14
55	*S*-Adenosylhomocysteine hydrolase	−2.10	−1.68	−1.25	63471580	6.1	48.08	MYL	35
56	SARDH	−2.16	−1.35	−1.59	26352359	6.4	57.84	CHO	37
57	SARDH	−2.80	−1.46	−1.92	26352359	6.4	57.84	CHO	37
58	SARDH	−6.43	−3.23	−1.99	26352359	6.4	57.84	CHO	37
59	SBP2	−3.66	−2.40	−1.53	188848341	5.8	53.16	XBM	25, 28
60	SBP2	+2.99	+1.63	+1.84	18848341	6.0	52.90	XBM	25, 28
61	Succinate dehydrogenase Fp subunit	−2.33	−1.81	−1.29	15030102	6.2	59.27	EGM	8
62	Transferrin	+2.83	+1.43	+1.98	62027488	7.0	78.87	APP	25
63	Transferrin	+4.17	+1.66	+2.52	62027488	7.0	78.87	APP	25
64	Transferrin	+4.72	+1.71	+2.76	62027488	7.0	78.87	APP	25
65	Transferrin	+4.60	+1.68	+2.74	62027488	7.0	78.87	APP	25
66	Tropomyosin 3	+2.19	+1.61	+1.37	26341416	4.7	27.88	STR	25, 46
67	Valosin-containing protein	+4.76	+3.68	+1.29	26350783	5.1	80.70	PRF	68
68	Vimentin	+2.31	+2.67	−1.16	31982755	4.9	53.73	STR	9, 25
69	Vimentin	+2.54	+2.68	−1.06	31982755	4.9	53.73	STR	9, 25
70	Aldehyde dehydrogenase A1	−2.62	−2.02	−1.41	32484332	8.3	55.08	ROX	17, 64
71	Catalase 1	−3.00	−2.61	−1.15	15004258	7.8	60.01	ROX	25, 48
72	Glutamate dehydrogenase	−2.76	−2.12	−1.30	26354278	8.6	61.60	EGM	42, 63
73	Glutathione *S*-transferase pi class	−3.27	−2.05	−1.59	2624496	8.3	23.52	XBM	25, 26
74	H2 Q4	+5.01	+3.23	−1.55	51770518	7.3	71.74	IMM	22, 29
75	H2 Q4	+8.09	+4.88	−1.66	51770518	7.3	71.74	IMM	22, 29
76	H2 Q4	+12.2	+7.29	−1.67	51770518	7.3	71.74	IMM	22, 29
77	H2 Q4	+18.3	+11.6	−1.58	51770518	7.3	71.74	IMM	22, 29
78	H2 Q4	+17.2	+10.4	−1.66	51770518	7.3	71.74	IMM	22, 29
79	*sm*-Phosphoenolpyruvate carboxykinase	+14.4	+8.05	−1.79	74828716	6.8	71.46	GLN	5
80	Prohibitin 2	+3.25	+1.61	+2.02	61556754 (76363295)	9.8	33.29	PRF	6, 41

[a] AVR: average volume ratio between study groups (C, control; M, MSS; H, HSS).
[b] APO, antiapoptotic; APP, acute-phase protein; CHO, choline metabolism; EGM, energy metabolism; GLN, gluconeogenesis; IMM, immune response; MYL, methylation; PHE, pheromone; PRF, protein folding; PRM, protein metabolism; ROX, redox reactions; SIG, cell signaling; STR, structural protein; XBM, xenobiotic metabolism.
[c] ATPS, ATP5 beta synthetase; DMDH, dimethylglycine dehydrogenase; EH, epoxide hydrolase; 10-FTHFDH, formyl tetrahydrofolate dehydrogenase; SARDH, sarcosine dehydrogenase; H2 Q4, MHC class I H2 Q4 alpha chain.

(%SBW) and gross pathological characteristics. The average percent spleen-to-body weight ratio for uninfected mice was 0.272, that for MSS mice was 0.578, and that for HSS mice was 2.314; these values are similar to those reported in previous studies (27).

2D-DIGE was used to measure the biological variation in protein abundance from uninfected and *S. mansoni*-infected animals with either MSS or HSS ($n = 5$ per group). This experiment was performed twice with independent sets of samples, and similar results were obtained for each replicate. Figure 1 is a pseudocolor map of superimposed DIGE images for pH 4 to 7 and pH 6 to 11 IPG strips and compares control liver lysate to a 20-week-infected HSS liver lysate. DeCyder software detected 2,550 spots each in the pH ranges of 4 to 7 and 6 to 11 by using the BVA module. The numbers of protein spots that changed for the pH ranges of 4 to 7 and 6 to 11 were 295 and 129, respectively. Furthermore, 134 and 38 protein spots in the pH ranges of 4 to 7 and 6 to 11 showed a ≥2-fold change in the average volume ratio, with an ANOVA value of ≤0.01. These were designated proteins of interest. The application of the false discovery rate (FDR) to eliminate false-positive results gave a total of 107 and 17 protein spots for each pH range, respectively. These 124 spots were subjected to MALDI-TOF mass fingerprinting and matched to database sequences, resulting in the identification of 80 protein spots (Fig. 1 and Table 1; see Table S2 in the supplemental material).

A previous study by our group used the 2DE approach to understand the impact of infection on 8-week *S. mansoni*-infected C57BL/6 mice and reported the impairment of multiple functional pathways in the liver during schistosomiasis (25). In a similar manner, we have assessed how the functional pathways were altered at 20 weeks of infection in CBA/J mice and compared the control mice with mice with MSS and HSS for changes that occurred (Fig. 2 and Table 1). In particular, we found that structural proteins, immune response proteins, and acute-phase proteins showed increased abundances, while the proteins related to energy metabolism, choline metabolism, and xenobiotic metabo-

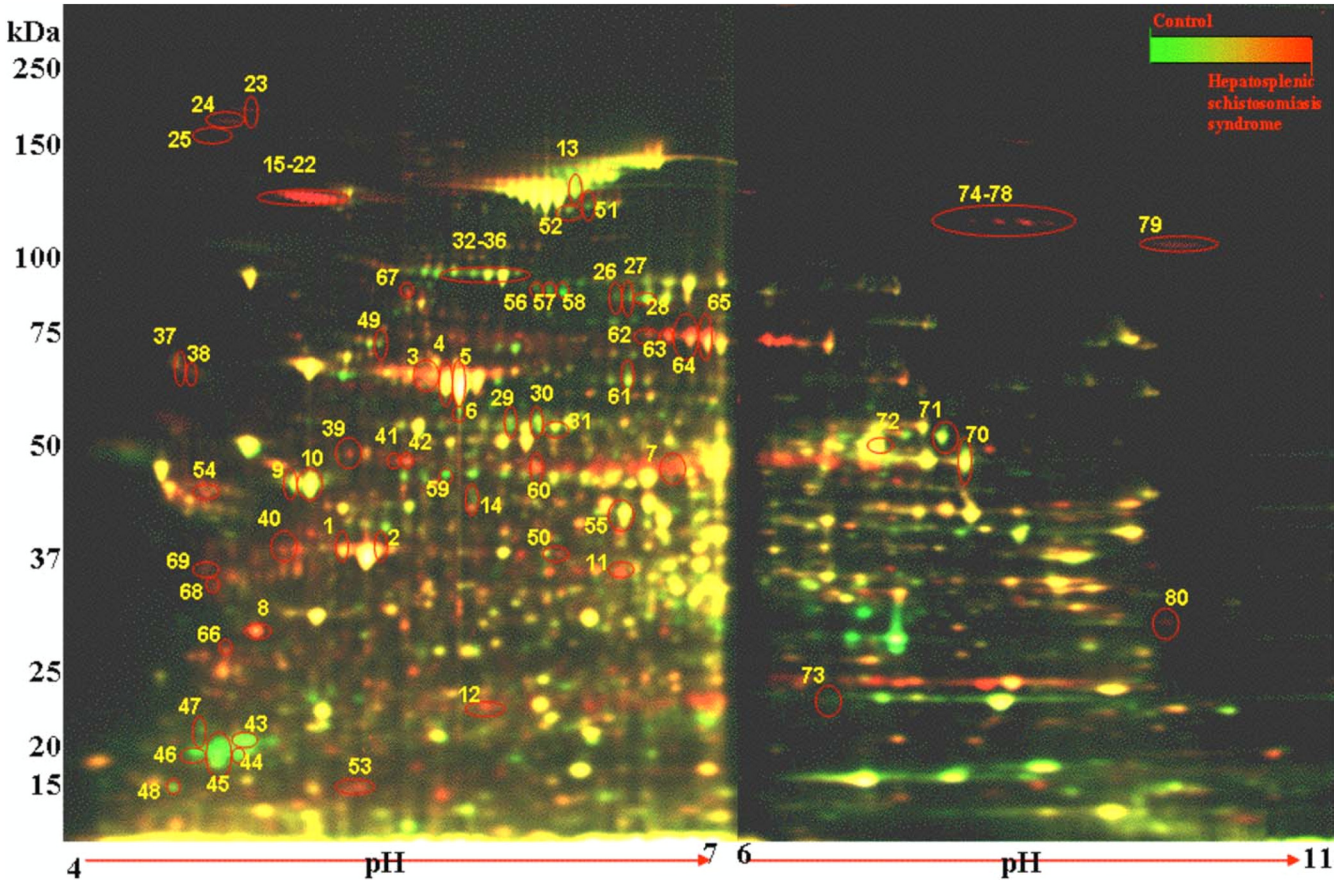

FIG. 1. Pseudocolor map of total liver proteins from uninfected and HSS mice separated by 2D-DIGE. Liver lysates from control/uninfected liver were labeled with Cy5 (green), lysates from 20-week-infected HSS liver were labeled with Cy3 (red), and a pooled internal standard of liver lysates from all mice in the study (n = 15) was labeled with Cy2 (blue) (not shown). Isoelectric focusing was performed on 7-cm IPG strips (pH 4 to 7 and pH 6 to 11), and proteins were then separated by using SDS-PAGE. The image overlays of Cy5- and Cy3-labeled proteins appear yellow. The numbers correspond to the protein spots in Table 1. Note that the MUP (protein spots 45 to 49) is green, showing higher abundance in control mice, and that collagen (protein spots 16 to 23) is red, showing higher abundance in HSS mice.

lism were decreased in abundance. Specific proteins of interest are discussed below.

Acute-phase protein: transferrin. Transferrin is a negative acute-phase protein, and decreased serum levels in patients with liver diseases were previously reported (45), while high levels are linked to alcoholic fatty liver disease (47). In patients with hepatosplenic schistosomiasis (51) and urinary schistosomiasis (4, 52), both increased (52) and decreased (4, 51) serum levels have been reported. Our previous work with C57BL/6 mice demonstrated increased liver transferrin levels after 8 weeks of *S. mansoni* infection (25). Similarly, this study shows a significant 2.5- to 4.6-fold increase in 4 transferrin spots (spots 62 to 65) (Fig. 1) in CBA/J mice with HSS but not MSS (Fig. 3 and Table 1) during the chronic stage of disease. The increased abundance of transferrin may be attributed to the growth of schistosome worms since a previous study found that schistosomes require iron and bind host transferrin for development (16). Our results suggest that increased levels of transferrin in HSS mice is a patent feature of that disease form and thus has potential as a biomarker for hepatosplenic disease.

Structural proteins. Intestinal and hepatosplenic schistosomiases are marked by fibrosis, which is the major cause of pathology and changes the structural composition of the liver. We found significant changes to two actins, gamma and beta actins (2-fold increase), and 11 collagens (2- to 55-fold increases) during schistosome infection (spots 1, 2, and 15 to 25) (Fig. 1 and Table 1). These findings support data from previous work (25), and the specific deposition of collagen isoforms 6a and XIV is consistent with previously documented liver fibrosis (19, 25). Another cytoskeletal protein, keratin D (type I) in mouse liver, corresponds to K18 (type I, acidic pI) in human liver and is associated with liver diseases (58). Using male Swiss Albino mice fed the fungistatic drug griseofulvin (53), Salmhofer et al. previously studied posttranslational modifications that were associated with the phosphorylation and proteolytic degradation of keratin filaments. Although that group investigated the structural disturbances caused by the modification of keratin in alcoholic hepatitis, our study shows that a similar protein change develops in severe schistosome-mediated liver pathology. Indeed, we found increased levels of keratin D associated with HSS but not MSS. This finding is unique to our study. Furthermore, research by Boehme et al. detected autoantibodies to keratin in patients with schistosomiasis infection (9), which, together with our findings, suggests

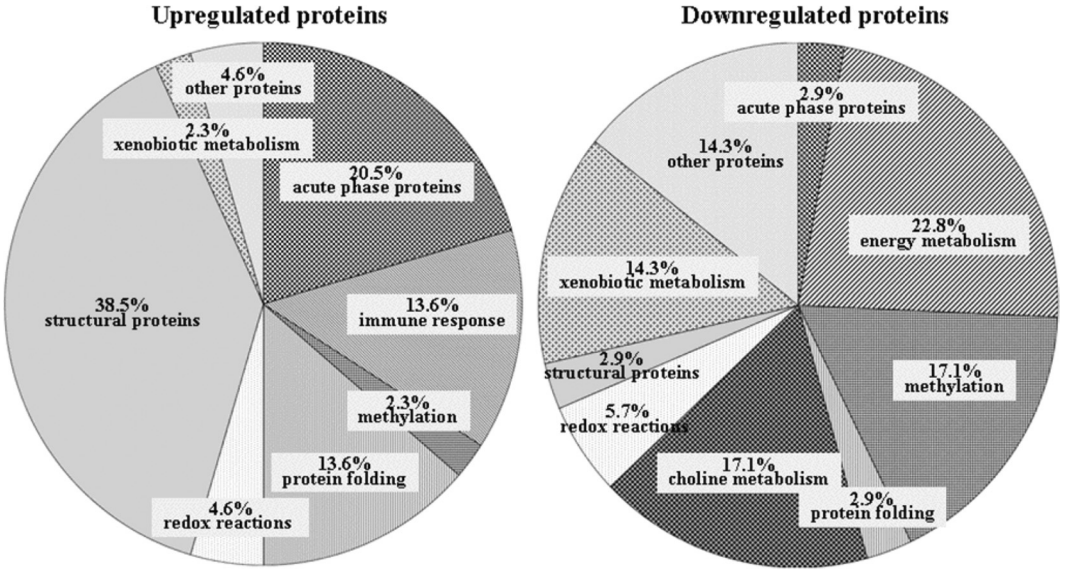

FIG. 2. Distribution of protein abundance during schistosomiasis by Gene Ontology molecular function categories.

that the development of a response to modified cytoskeletal proteins such as keratin may contribute to disease pathology.

Energy metabolism. Schistosomiasis causes liver dysfunction and the disruption of major metabolic pathways, including proteins involved in energy and nitrogen metabolism such as the ATP synthase beta subunit, carbamoyl phosphate synthase 1, and pyruvate carboxylase. The ATP synthase beta subunit is a mitochondrial respiratory chain component of the ATP synthesis complex and is involved in liver regeneration (11). We found significant decreases in levels of this enzyme during chronic HSS schistosomiasis, consistent with previous results for mice with acute infections (25). Carbamoyl phosphate synthase 1 is a urea cycle enzyme that is associated with liver carcinogenesis and hepatotoxicity. Likewise, the level of this enzyme was decreased in mice with HSS (25, 60). The level of pyruvate carboxylase, a gluconeogenic enzyme that was previously reported to have decreased levels in rat and human hepatomas (24) and in schistosomiasis (25), was also decreased. The reduction of these protein spots by 2- to 3-fold is suggestive of changes in liver metabolism during the development of the more severe 20-week schistosome-mediated liver pathology.

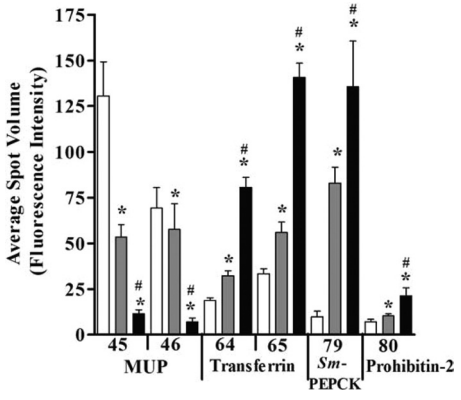

FIG. 3. The abundances of MUP isoforms, transferrin isoforms, *Sm*PEPCK, and prohibitin 2 are significantly altered in HSS livers. One-way ANOVA for all spots gave a P value of ≤ 0.01. *, $P < 0.05$ compared to control; #, $P < 0.05$ compared to MSS mice by Newman-Keuls multiple-comparison test. The numbers on the x axis correspond to the protein spots in Table 1.

Choline metabolism. We found a significant decrease in the abundances of two proteins associated with choline metabolism, dimethylglycine dehydrogenase (DMDH) and sarcosine dehydrogenase (SARDH). These mitochondrial dehydrogenases catalyze the final steps of choline metabolism, converting dimethylglycine to sarcosine and then sarcosine to glycine. The predicted native masses of the proteins are 97.3 and 101.7 kDa for DMDH and SARDH, respectively, corresponding to their positions on the gels. Both proteins have predicted posttranslational modifications including phosphorylation that would potentially give rise to isoforms that differ in their isoelectric points. In HSS livers, three DMDH spots (spots 26 to 28) (Fig. 1) showed a greater-than-2-fold loss, with a smaller nonsignificant decrease in MSS compared to controls (Table 1). The levels of three SARDH isoforms (spots 56 to 58) also decreased more than 2-fold in HSS, with smaller decreases in MSS. The greatest loss of more than 6-fold in HSS mice was for the most basic (spot 58) of the three SARDH isoforms. The loss of DMDH is similar to the findings described previously by Harvie et al. (25), and the loss of SARDH was reported previously for hepatocellular carcinoma (37). Our research found 2- to 6.4-fold decreases in the SARDH spots, suggesting similar hepatic responses in schistosomiasis and hepatocarcinogenesis. Furthermore, SARDH may be useful to differentiate between HSS and MSS, since the average volume ratio decrease for three SARDH spots in HSS is large in comparison to that in MSS, which is suggestive of an isoform pattern specific for severe disease. Additionally, schistosomes use host lipids for survival, as they do not make sterols or fatty acids *de*

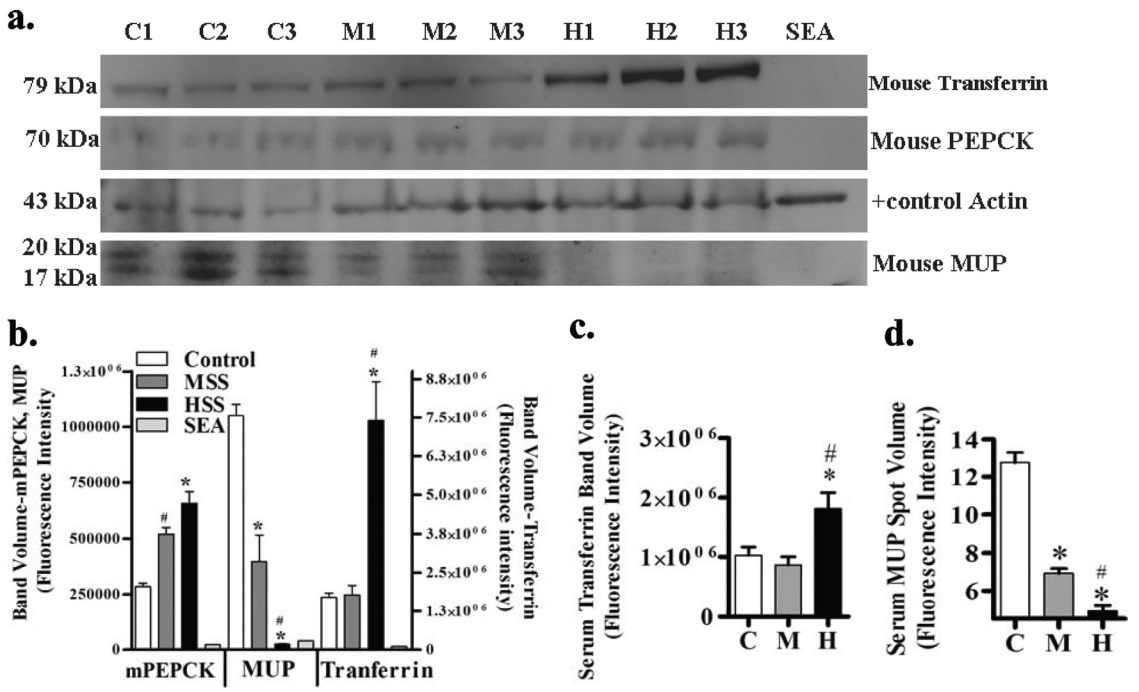

FIG. 4. Western blot analysis of MUP, PEPCK, and transferrin. (a) Lysates (20 μg/well) from control (C) ($n = 3$), MSS (M) ($n = 3$), and HSS (H) ($n = 3$), liver samples and soluble egg antigen (SEA; 20 μg/well) were separated on an SDS-PAGE gel, transferred onto a PVDF membrane, and probed with rabbit anti-murine PEPCK (mPEPCK) polyclonal antibody, goat anti-MUP, goat anti-transferrin polyclonal antibody, or mouse anti-actin monoclonal antibody as a loading control, followed by Cy5-labeled anti-goat IgG, anti-rabbit IgG, and Cy3-labeled anti-mouse IgG. (b) Protein band fluorescence intensity of HSS mouse liver lysate compared with control and MSS mouse liver lysate. Shown are the means ± standard errors of the means (SEM). *, $P < 0.05$ compared to control; #, $P < 0.05$ compared to MSS mice by Newman-Keuls multiple-comparison test. (c) Mouse serum transferrin (1:50 serum dilution of a 10-μg/μl sample with phosphate-buffered saline [pH 7.4]) from control ($n = 5$), MSS ($n = 5$), and HSS ($n = 5$) mice separated on an SDS-PAGE gel, transferred onto a PVDF membrane, and probed with goat anti-transferrin polyclonal antibody followed by Cy5-labeled anti-goat IgG. The protein band fluorescence intensity of HSS sera was compared with those for control and MSS sera for serum transferrin. The one-way ANOVA P value was ≤0.01 for all band volumes. *, $P < 0.05$ compared to control; #, $P < 0.05$ compared to MSS mice by Newman-Keuls multiple-comparison test. (d) Mouse serum MUP spot data from serum DIGE. One-way ANOVA for all spots gave a P value of ≤0.01. Newman-Keuls multiple-comparison test compared HSS mice to control and MSS mice with a P value of <0.05.

novo. Choline is crucial for phosphatidylcholine biosynthesis in schistosome development, especially in female worms (3). The decreased levels of SARDH and DMDH reported in our study could mean increased choline uptake toward phosphatidylcholine biosynthesis.

Xenobiotic metabolism. Schistosome infection induces alterations in the redox balance due to increases in numbers of schistosome eggs in the host liver microvasculature that cause oxidative stress from immune-generated radicals (34). Moreover, the release of toxic heme and ferrous ions generated due to the consumption of hemoglobin by schistosome larvae (10) contributes to the increase in amounts of xenobiotic proteins. In contrast, the xenobiotic proteins identified in our study showed decreased amounts (Fig. 2 and Table 1). The glutathione *S*-transferase (GST) enzyme family is associated with the detoxification of endogenous and exogenous toxins. Increased levels of glutathione *S*-transferase class pi (GSTPi) in tumor tissues (26) as well as in schistosomiasis (25) were previously reported. In contrast, our study found decreased levels of GSTPi (spot 73) in MSS and HSS mice, and this decrease may represent alterations in protein abundance during the chronic stage of infection compared to the acute stage.

Selenium binding protein 2 (SBP2) is a liver protein that has anticancer and neuroprotective properties (15, 21). Henkel et al. previously used carbon tetrachloride to induce liver fibrosis and portal hypertension in BALB/c mice and found that the level of SBP2 was decreased by using DIGE techniques (28). Similar to these findings and those described previously by Harvie et al. using schistosome-infected mice (25), our research shows decreased levels of SBP2 (spot 59) (Table 1) in HSS mice by 3.5-fold and in MSS mice by 2.5-fold. However, we also report one upregulated SBP2 spot (spot 60) (Table 1) in HSS. While this finding seems contradictory, it indicates that a more in-depth analysis of different SBP2 isoforms may provide a better perspective of the involvement of these isoforms in schistosomiasis and determine their relevance as specific biomarkers.

Immune-related proteins. Schistosome eggs are well-characterized inducers of immune responses (27). In MSS and HSS mice, there was a 2- to 18-fold elevation of the level of the major histocompatibility complex (MHC) class I histocompatibility antigen H2 Q4 alpha chain precursor, a nonclassical MHC class Ib-like molecule (spots 74 to 78). This upregulation may reflect an increased or altered immune recognition of parasite-derived products. While Hernandez et al. showed that classical MHC class II, but not MHC class I, molecules are

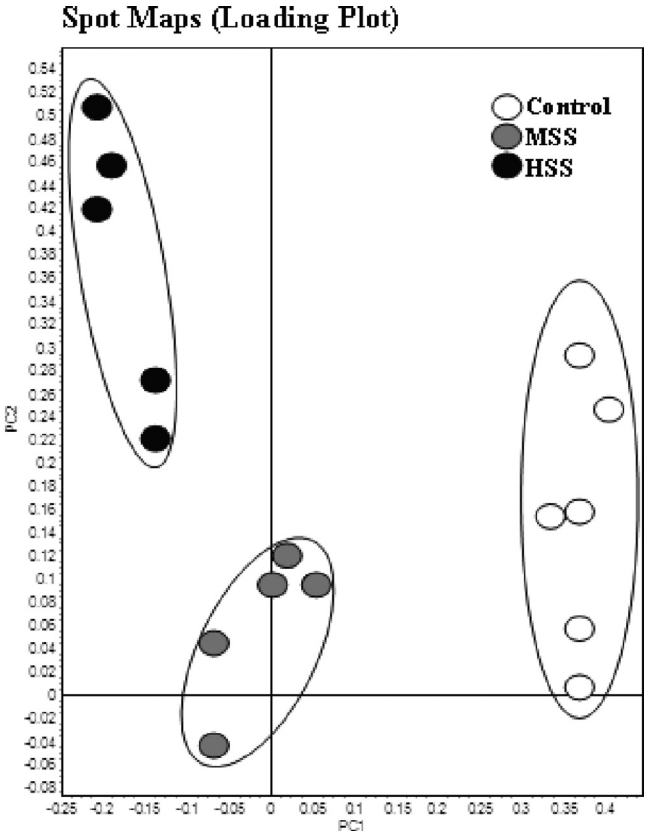

FIG. 5. Principal-component analysis plot for pH 4 to 7 spots with a 2-fold change and ANOVA value of ≤0.01. Spot maps (2D-DIGE images) show the best separation of moderate and severe disease from control (uninfected) CBA/J mice.

involved in granuloma formation in early-stage disease (29), our data suggest a possible role for the nonclassical MHC molecules like H2 Q4 in the development of schistosome-induced immune responses.

Levels of two other immune-related proteins, lymphocyte cytosolic protein 1 and prohibitin 2, were significantly increased in chronically infected mice. Lymphocyte cytosolic protein 1 (plastin 2) is an actin-binding protein expressed in monocytes, B lymphocytes, and myeloid cells. A recent study showed an increased abundance of lymphocyte cytosolic protein 1 in chemically induced mouse liver tumors (57), and another study reported a 3-fold increase of lymphocyte cytosolic protein 1 transcript levels using Affymetrix microarray profiling in C57BL/6J mice with traumatic brain injury (30). Although the technique, mouse model, and tissue studied differ, we report similar findings with two lymphocyte cytosolic protein 1 spots (spots 41 and 42) (Table 1) showing an increased protein abundance (3- to 4-fold). Taken together, we believe that increased levels of this protein are associated with tissue injury and stress conditions and suggest effects on stress metabolism in moderate and severe schistosomiasis.

Prohibitin 2 (B-cell receptor-associated protein 37) is closely related to and complexed with prohibitin 1 (p32). It plays a role in tumor suppression and cell cycle regulation as well as inducing apoptosis (23). Because the level of prohibitin gene expression increases in rat bladder carcinomas and it interacts with tumor suppressor gene proteins (6), it was highlighted as a possible therapeutic target (41). Our study shows a significant 3.25-fold increase in HSS but not MSS mice (spot 80) (Table 1 and Fig. 3) and may indicate its involvement in cell proliferation and/or apoptosis during severe disease. Furthermore, it provides further support for the idea that similar pathological mechanisms may be occurring during schistosome-mediated liver disease and carcinogenesis.

Major urinary protein and phosphoenolpyruvate carboxykinase. Major urinary protein (MUP) is from the lipocalin family and functions as a pheromone transporter in mouse urine. MUP has similarity to human epididymis-specific lipocalin 9, but more elaborate studies are needed to understand the relationship between this protein in mice and that in humans (65). Previous research suggested that a decrease in MUP levels is an early event in the development of mouse liver tumors and may be used as a tumor marker in mouse hepatocarcinogenesis (18). Our study shows five MUP spots (spots 43 to 47) (Table 1) with a 2- to 10-fold decrease in expression levels specifically in HSS livers, while MSS livers showed only two spots with a 2.6-fold decrease in expression levels. This is the first report of a specific alteration in this protein during schistosomiasis (Fig. 3 and Table 1). The large decrease of MUP levels in HSS livers lends further support to the possibility of early-stage responses to hepatocarcinogenesis having similarities to hepatosplenic schistosomiasis.

Asahi et al. previously proposed that *S. mansoni* phosphoenolpyruvate carboxykinase (*Sm*PEPCK) is a novel antigen for schistosome infection and suggested its potential as a disease-specific protein marker (5). In agreement with those findings, we found that *Sm*PEPCK abundance increased >13-fold in HSS livers and 8-fold in MSS livers (spot 79) (Table 1 and Fig. 3). While mice do express a murine PEPCK, the results from the proteomic analyses have matched the protein spot to the parasite and not mouse PEPCK. Thus, due to the large increase in amounts of *Sm*PEPCK in our study, we agree with the conclusions of Asahi et al. that this protein is a good candidate for development as a biomarker for schistosome infection.

Protein abundance verification. To verify the huge changes in the abundance of *Sm*PEPCK, mouse MUP, and mouse transferrin, we performed Western blot analysis of liver lysates and serum samples from uninfected, MSS, and HSS mice (Fig. 4a and b). Liver lysates from 3 mice per group were analyzed and probed for the expression of MUP, PEPCK, transferrin, or actin as a loading control. The antibody used to detect PEPCK was known to recognize mouse PEPCK, but its reactivity to *Sm*PEPCK was unknown, and thus, we included soluble schistosome egg antigen (SEA) to test its specificity. Although there was no reaction with the schistosome protein, increases in levels of PEPCK were observed for MSS and HSS liver lysates (Fig. 4a and b). This indicated that in addition to the increase in *Sm*PEPCK detected by DIGE, the mouse liver enzyme also increased in abundance. Furthermore, the PEPCK results indicate that there is a potential for enhanced gluconeogenesis in infected liver through the increased activity of this hepatic enzyme. PEPCK also has a role in glucose metabolism in schistosomes, as PEPCK carboxylates phosphoenolpyruvate to oxaloacetate that is then converted to malate for the parasite's

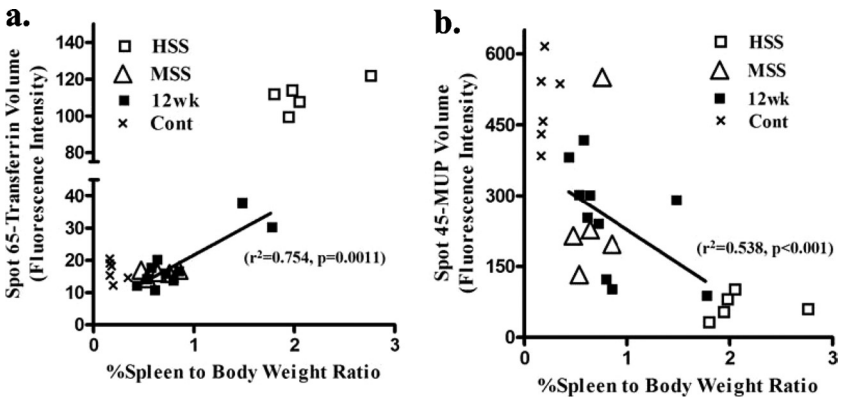

FIG. 6. Comparison of spot volume fluorescence intensities from liver MUP spot 45 (a) and liver transferrin spot 65 (b) with percent spleen-to-body weight ratios from control and 12-week-infected MSS and HSS mice. Linear regression analysis for 12-week-infected mice ($n = 10$) gave the following values: r^2 of 0.538 and P value of <0.001 for MUP and r^2 of 0.754 and P value of 0.0011 for transferrin.

energy needs (39). These results suggest that levels of PEPCK of mouse origin as well as *Sm*PEPCK increase in MSS and HSS mice and that further studies are needed to target *Sm*PEPCK specifically.

In contrast to *Sm*PEPCK, our 2D-DIGE results indicated that both transferrin and MUP changes were greater for HSS mice. Using Western blotting, we found that the MUP band intensity for MSS mice and especially HSS mice was decreased compared to that for control mice (Fig. 4b). In contrast, the transferrin protein band intensity for HSS mice was significantly higher than those for both MSS and control mice (Fig. 4b). These results verify our 2D-DIGE findings for the MUP and transferrin abundance in the liver (Fig. 1 and 4b). To determine if the difference in transferrin expression levels was reflected in serum, we assessed serum transferrin levels by Western blotting and found a significant increase for HSS mice compared to MSS and control mice (Fig. 4c). In addition, 2D-DIGE confirmed that the level of serum MUP was significantly decreased in HSS mice compared to that in MSS and control mice (Fig. 4d). Together, these findings indicate that the differences in liver abundance of transferrin and MUP are reflected in the serum and are markers for chronic hepatosplenic disease in mice.

Multivariate analysis. Principal-component analysis was used to compare the protein spot map data from the three study groups. This supervised analysis showed a close clustering of the individual 2D-DIGE spot maps within each group and thus revealed that control, MSS, and HSS mice have distinct and unique liver protein patterns (Fig. 5 and see Fig. S1 in the supplemental material). Hierarchical cluster analysis is an unsupervised multivariate analysis depicted by a dendrogram and heat map; this analysis gave an overview of the different proteins and study groups with similar expression profiles grouped together (see Fig. S2 and S3 in the supplemental material). As seen on the left-hand side of the heat map, the proteins with similar functional groups are clustered together, while the 2D-DIGE spot maps with similar levels of protein expression are segregated into experimental groups, as stated in our study. Taken together, the results of the supervised and unsupervised multivariate analyses indicate that MSS and HSS mice have distinct proteomic signatures that reflect the pathology of schistosomiasis, and further analysis of the unique protein changes may provide insight into the molecular changes that drive these disease forms.

Protein abundance and disease severity. We explored the relationship between the percent spleen-to-body weight ratio (%SBW) and transferrin and MUP abundances. We found a significant correlation between the change in MUP and transferrin abundances and %SBW for control, MSS, and HSS mice (Fig. 6). To further understand if this relationship was apparent at an earlier time point after infection, we compared the liver spot volumes of MUP and transferrin of 12-week-infected mice ($n = 10$) with their %SBW and found that the expression of these two proteins correlated with disease severity (Fig. 6). Associations between %SBW and MUP and transferrin were tested by using simple linear regression. There were significant correlations with disease severity ($r^2 = 0.538$ and $P < 0.001$ for MUP and $r^2 = 0.754$ and $P = 0.0011$ for transferrin). Overall, these results show that the unique liver protein changes that distinguish HSS and MSS correlate to pathology and are detectable during the early chronic stage of disease.

The use of the CBA/J mouse chronic experimental schistosomiasis model allowed us to explore the physiological roles and biochemical activities of various protein isoforms and variants associated with MSS and HSS disease forms. The liver 2D-DIGE profiles depicted a unique picture of protein patterns expressed between MSS and HSS and revealed an increased abundance of proteins associated with energy metabolism, choline metabolism, and xenobiotic metabolism. The uniqueness of this study lies in the fact that lymphocyte cytosolic protein 1 isoforms, sarcosine dehydrogenase isoforms, prohibitin 2, transferrin isoforms, and MUP have not previously been associated with hepatosplenic schistosomiasis. Furthermore, we were able to verify that changes in transferrin and MUP levels in the liver were reflected in the serum and that these changes correlated with disease severity even at early time points. Thus, we believe that these proteins may be valuable as potential diagnostic biomarkers that may assist in the early detection and treatment of schistosomiasis patients.

ACKNOWLEDGMENTS

This work was supported by funds from the University Research Fund and Wellington Medical Research Foundation.

We thank Danyl McLauchlan, Pete Augostini, and Nokuthaba Sibanda for precious advice and assistance.

The findings and conclusions in this report are those of the authors and do not necessarily represent the views of the CDC.

REFERENCES

1. **Agaton, C., J. Galli, I. H. Guthenberg, L. Janzon, M. Hansson, A. Asplund, E. Brundell, S. Lindberg, I. Ruthberg, K. Wester, D. Wurtz, C. Höög, J. Lundeberg, S. Ståhl, F. Pontén, and M. Uhlén.** 2003. Affinity proteomics for systematic protein profiling of chromosome 21 gene products in human tissues. Mol. Cell. Proteomics **2:**405–414.
2. **Altmann, F.** 2007. The role of protein glycosylation in allergy. Int. Arch. Allergy Immunol. **142:**99–115.
3. **Ancelin, M. L., G. Torpier, H. J. Vial, and A. Capron.** 1987. Choline incorporation by *Schistosoma mansoni*: distribution of choline metabolites during development and after sexual differentiation. J. Parasitol. **73:**530–535.
4. **Arinola, O. G.** 2004. Metal binding acute phase proteins and trace elements in Nigerian children with urinary schistosomiasis. Biokemistri **16:**23–27.
5. **Asahi, H., A. Osman, R. M. Cook, P. T. LoVerde, and M. J. Stadecker.** 2000. *Schistosoma mansoni* phosphoenolpyruvate carboxykinase, a novel egg antigen: immunological properties of the recombinant protein and identification of a T-cell epitope. Infect. Immun. **68:**3385–3393.
6. **Asamoto, M., and S. M. Cohen.** 1994. Prohibitin gene is overexpressed but not mutated in rat bladder carcinomas and cell lines. Cancer Lett. **83:**201–207.
7. **Beddek, A. J., P. Rawson, L. Peng, R. Snell, K. Lehnert, H. E. Ward, and T. W. Jordan.** 2008. Profiling the metabolic proteome of bovine mammary tissue. Proteomics **8:**1502–1515.
8. **Blanc, J., C. Lalanne, C. Plomion, J. Schmitter, K. Bathany, J. Gion, P. Bioulac-Sage, C. Balabaud, M. Bonneu, and J. Rosenbaum.** 2005. Proteomic analysis of differentially expressed proteins in hepatocellular carcinoma developed in patients with chronic viral hepatitis C. Proteomics **5:**3778–3789.
9. **Boehme, M. W. J., P. K. Kataaha, and E. J. Holborow.** 1989. Autoantibodies to intermediate filaments in sera of patients with Schistosoma mansoni infection. Clin. Exp. Immunol. **77:**230–233.
10. **Brindley, P. J., B. H. Kalinna, J. P. Dalton, S. R. Day, J. Y. M. Wong, M. L. Smythe, and D. P. McManus.** 1997. Proteolytic degradation of host hemoglobin by schistosomes. Mol. Biochem. Parasitol. **89:**1–9.
11. **Capuano, F., F. Guerrieri, and S. Papa.** 1997. Oxidative phosphorylation enzymes in normal and neoplastic cell growth. J. Bioenerg. Biomembr. **29:**379–384.
12. **Chen, H. B., K. Pan, M. K. Tang, Y. L. Chui, L. Chen, Z. J. Su, Z. Y. Shen, E. M. Li, W. Xie, and K. K. H. Lee.** 2008. Comparative proteomic analysis reveals differentially expressed proteins regulated by a potential tumor promoter, BRE, in human esophageal carcinoma cells. Biochem. Cell Biol. **86:**302–311.
13. **Chitsulo, L., D. Engels, A. Montresor, and L. Savioli.** 2000. The global status of schistosomiasis and its control. Acta Trop. **77:**41–51.
14. **Chu, P., J. Pardo, H. Zhao, C. C. Li, E. Pali, M. M. Shen, K. Qu, S. X. Yu, B. C. B. Huang, P. Yu, E. S. Masuda, S. M. Molineaux, F. Kolbinger, G. Aversa, J. De Vries, D. G. Payan, and X. C. Liao.** 2003. Systematic identification of regulatory proteins critical for T-cell activation. J. Biol. **2:**211–2116.
15. **Chu, R., H. Lim, L. Brumfield, H. Liu, C. Herring, P. Ulintz, J. K. Reddy, and M. Davison.** 2004. Protein profiling of mouse livers with peroxisome proliferator-activated receptor alpha activation. Mol. Cell. Biol. **24:**6288–6297.
16. **Clemens, L. E., and P. F. Basch.** 1989. *Schistosoma mansoni*: effect of transferrin and growth factors on development of schistosomula in vitro. J. Parasitol. **75:**417–421.
17. **Dragani, T. A., F. S. Falvella, G. Manenti, M. A. Pierotti, and R. A. Gambetta.** 1996. Downexpression of aldehyde dehydrogenase 1 in murine lung tumors. Mol. Carcinog. **16:**123–125.
18. **Dragani, T. A., G. Manenti, M. R. M. Sacchi, B. M. Colombo, and G. Della Porta.** 1989. Major urinary protein as a negative tumor marker in mouse hepatocarcinogenesis. Mol. Carcinog. **2:**355–360.
19. **Dunn, M. A., R. Kamel, and I. A. Kamel.** 1979. Liver collagen synthesis in schistosomiasis mansoni. Gastroenterology **76:**978–982.
20. **Forestier, M., R. Bänninger, J. Reichen, and M. Solioz.** 2003. Betaine homocysteine methyltransferase: gene cloning and expression analysis in rat liver cirrhosis. Biochim. Biophys. Acta **1638:**29–34.
21. **Giometti, C. S., X. Liang, S. L. Tollaksen, D. B. Wall, D. M. Lubman, V. Subbarao, and M. S. Rao.** 2000. Mouse liver selenium-binding protein decreased in abundance by peroxisome proliferators. Electrophoresis **21:**2162–2169.
22. **Grzych, J. M., E. Pearce, A. Cheever, Z. A. Caulada, P. Caspar, S. Heiny, F. Lewis, and A. Sher.** 1991. Egg deposition is the major stimulus for the production of Th2 cytokines in murine schistomiasis mansoni. J. Immunol. **146:**1322–1327.
23. **Guo, W., H. Xu, J. Chen, Y. Yang, J. W. Jin, R. Fu, H. M. Liu, X. L. Zha, Z. G. Zhang, and W. Y. Huang.** 2007. Prohibitin suppresses renal interstitial fibroblasts proliferation and phenotypic change induced by transforming growth factor-β1. Mol. Cell. Biochem. **295:**167–177.
24. **Hammond, K. D., and D. Balinsky.** 1978. Activities of key gluconeogenic enzymes and glycogen synthase in rat and human livers, hepatomas, and hepatoma cell cultures. Cancer Res. **38:**1317–1322.
25. **Harvie, M., T. W. Jordan, and A. C. La Flamme.** 2007. Differential liver protein expression during schistosomiasis. Infect. Immun. **75:**736–744.
26. **Hayes, P. C., L. May, J. D. Hayes, and D. J. Harrison.** 1991. Glutathione S-transferases in human liver cancer. Gut **32:**1546–1549.
27. **Henderson, G. S., N. A. Nix, M. A. Montesano, D. Gold, G. L. Freeman, Jr., T. L. McCurley, and D. G. Colley.** 1993. Two distinct pathological syndromes in male CBA/J inbred mice with chronic *Schistosoma mansoni* infections. Am. J. Pathol. **142:**703–714.
28. **Henkel, C., M. Roderfeld, R. Weiskirchen, M. L. Berres, S. Hillebrandt, F. Lammert, H. E. Meyer, K. Stühler, J. Graf, and E. Roeb.** 2006. Changes of the hepatic proteome in murine models for toxically induced fibrogenesis and sclerosing cholangitis. Proteomics **6:**6538–6548.
29. **Hernandez, H. J., Y. Wang, N. Tzellas, and M. J. Stadecker.** 1997. Expression of class II, but not class I, major histocompatibility complex molecules is required for granuloma formation in infection with Schistosoma mansoni. Eur. J. Immunol. **27:**1170–1176.
30. **Israelsson, C., H. Bengtsson, A. Kylberg, K. Kullander, A. Lewén, L. Hillered, and T. Ebendal.** 2008. Distinct cellular patterns of upregulated chemokine expression supporting a prominent inflammatory role in traumatic brain injury. J. Neurotrauma **25:**959–974.
31. **Karp, N. A., and K. S. Lilley.** 2005. Maximising sensitivity for detecting changes in protein expression: experimental design using minimal CyDyes. Proteomics **5:**3105–3115.
32. **Karp, N. A., M. Spencer, H. Lindsay, K. O'Dell, and K. S. Lilley.** 2005. Impact of replicate types on proteomic expression analysis. J. Proteome Res. **4:**1867–1871.
33. **Krupenko, S. A., and N. V. Oleinik.** 2002. 10-Formyltetrahydrofolate dehydrogenase, one of the major folate enzymes, is down-regulated in tumor tissues and possesses suppressor effects on cancer cells. Cell Growth Differ. **13:**227–236.
34. **La Flamme, A. C., E. A. Patton, B. Bauman, and E. J. Pearce.** 2001. IL-4 plays a crucial role in regulating oxidative damage in the liver during schistosomiasis. J. Immunol. **166:**1903–1911.
35. **Leal, J. F., I. Ferrer, C. Blanco-Aparicio, J. Hernandez-Losa, C. S. Ramony, A. Carnero, and M. E. Lleonart.** 2008. *S*-Adenosylhomocysteine hydrolase downregulation contributes to tumorigenesis. Carcinogenesis **29:**2089–2095.
36. **Li, Q., A. K. Ching, B. C. Chan, S. K. Chow, P. Lim, T. C. Ho, W. Ip, C. Wong, C. W. Lam, K. K. Lee, J. Y. Chan, and Y. Chui.** 2004. A death receptor-associated anti-apoptotic protein, BRE, inhibits mitochondrial apoptotic pathway. J. Biol. Chem. **279:**52106–52116.
37. **Lim, S. O., S. Park, W. Kim, S. G. Park, H. Kim, Y. Kim, T. Sohn, J. Noh, and G. Jung.** 2002. Proteome analysis of hepatocellular carcinoma. Biochem. Biophys. Res. Commun. **291:**1031–1037.
38. **Magnussen, P.** 2003. Treatment and re-treatment strategies for schistosomiasis control in different epidemiological settings: a review of 10 years' experiences. Acta Trop. **86:**243–254.
39. **Mehlhorn, H.** 2009. Energy metabolism. *In* H. Mehlhorn (ed.), Parasitology research & encyclopedic reference of parasitology, 2nd ed. Springer-Verlag, Heidelberg, Germany. http://parasitology.informatik.uni-wuerzburg.de.
40. **Meier, U., O. Gressner, F. Lammert, and A. M. Gressner.** 2006. Gc-globulin: roles in response to injury. Clin. Chem. **52:**1247–1253.
41. **Mishra, S., L. C. Murphy, B. L. G. Nyomba, and L. J. Murphy.** 2005. Prohibitin: a potential target for new therapeutics. Trends Mol. Med. **11:**192–197.
42. **Morand, J. F., J. Macri, and K. Adeli.** 2005. Proteomic profiling of hepatic endoplasmic reticulum-associated proteins in an animal model of insulin resistance and metabolic dyslipidemia. J. Biol. Chem. **280:**17626–17633.
43. **Mulla, A., H. C. Christian, E. Solito, N. Mendoza, J. F. Morris, and J. C. Buckingham.** 2004. Expression, subcellular localization and phosphorylation status of annexins 1 and 5 in human pituitary adenomas and a growth hormone-secreting carcinoma. Clin. Endocrinol. **60:**107–119.
44. **Murray, G. I., P. J. Paterson, R. J. Weaver, S. W. B. Ewen, W. T. Melvin, and M. D. Burke.** 1993. The expression of cytochrome P-450, epoxide hydrolase, and glutathione S-transferase in hepatocellular carcinoma. Cancer **71:**36–43.
45. **Otegbayo, J. A., O. G. Arinola, A. Aje, O. A. Oluwasola, O. H. Okiwelu, and L. S. Salimonu.** 2005. Usefulness of acute phase proteins for monitoring development of hepatocellular carcinoma in hepatitis B virus carriers. West Afr. J. Med. **24:**124–127.
46. **Otogawa, K., T. Ogawa, R. Shiga, K. Ikeda, and N. Kawada.** 2009. Induction of tropomyosin during hepatic stellate cell activation and the progression of liver fibrosis. Hepatol. Int. **3:**378–383.
47. **Potter, B. J., R. W. G. Chapman, R. M. Nunes, D. Sorrentino, and S.**

Sherlock. 1985. Transferrin metabolism in alcoholic liver disease. Hepatology **5:**714–721.
48. **Rizk, M., T. A. Fayed, M. Badawy, and N. S. El-Regal.** 2006. Effect of different durations of *Schistosoma mansoni* infection on the levels of some antioxidants in mice. Med. J. Islam. World Acad. Sci. **16:**25–34.
49. **Rudd, P. M., T. Elliott, P. Cresswell, I. A. Wilson, and R. A. Dwek.** 2001. Glycosylation and the immune system. Science **291:**2370–2376.
50. Reference deleted.
51. **Saif, M., J. Tawfik, M. A. Ali, S. F. El-Mahrouky, N. Galil, and M. N. Galal.** 1977. Serum transferrin, albumin and IgG levels in hepatosplenic bilharziasis in Egypt. J. Egypt. Med. Assoc. **60:**731–743.
52. **Salawu, L., and O. G. Arinola.** 2004. Acute phase proteins in pregnant women with urinary schistosomiasis in live villages, Osun State, Nigeria. Afr. J. Biomed. Res. **7:**103–106.
53. **Salmhofer, H., I. Rainer, K. Zatloukal, and H. Denk.** 1994. Posttranslational events involved in griseofulvin-induced keratin cytoskeleton alterations. Hepatology **20:**731–740.
54. **Santos, S. G., E. C. Campbell, S. Lynch, V. Wong, A. N. Antoniou, and S. J. Powis.** 2007. Major histocompatibility complex class I-ERp57-tapasin interactions within the peptide-loading complex. J. Biol. Chem. **282:**17587–17593.
55. **Schiødt, F. V.** 2008. Gc-globulin in liver disease. Dan. Med. Bull. **55:**131–146.
56. **Stadecker, M. J.** 1999. The development of granulomas in schistosomiasis: genetic backgrounds, regulatory pathways, and specific egg antigen responses that influence the magnitude of disease. Microbes Infect. **1:**505–510.
57. **Strathmann, J., K. Paal, C. Ittrich, E. Krause, K. E. Appel, H. P. Glauert, A. Buchmann, and M. Schwarz.** 2007. Proteome analysis of chemically induced mouse liver tumors with different genotype. Proteomics **7:**3318–3331.
58. **Strnad, P., C. Stumptner, K. Zatloukal, and H. Denk.** 2008. Intermediate filament cytoskeleton of the liver in health and disease. Histochem. Cell Biol. **129:**735–749.
59. **Sun, W., B. Xing, Y. Sun, X. Du, M. Lu, C. Hao, Z. Lu, W. Mi, S. Wu, H. Wei, X. Gao, Y. Zhu, Y. Jiang, X. Qian, and F. He.** 2007. Proteome analysis of hepatocellular carcinoma by two-dimensional difference gel electrophoresis. Mol. Cell. Proteomics **6:**1798–1808.
60. **Thome-Kromer, B., M. K. I. Bonk, G. Nebrich, M. Taufmann, S. Bryant, U. Wacker, and A. Köpke.** 2003. Towards the identification of liver toxicity markers: a proteome study in human cell culture and rats. Proteomics **3:**1835–1862.
61. **Uchio, K., B. Tuchweber, N. Manabe, G. Gabbiani, J. Rosenbaum, and A. Desmouliere.** 2002. Cellular retinol-binding protein-1 expression and modulation during in vivo and in vitro myofibroblastic differentiation of rat hepatic stellate cells and portal fibroblasts. Lab. Invest. **82:**619–628.
62. **Van der Werf, M. J., S. J. De Vlas, S. Brooker, C. W. N. Looman, N. J. D. Nagelkerke, J. D. F. Habbema, and D. Engels.** 2003. Quantification of clinical morbidity associated with schistosome infection in sub-Saharan Africa. Acta Trop. **86:**125–139.
63. **Van Waes, L., and C. S. Lieber.** 1977. Glutamate dehydrogenase: a reliable marker of liver cell necrosis in the alcoholic. Br. Med. J. **ii:**1508–1510.
64. **Vasiliou, V., A. Pappa, and D. R. Petersen.** 2000. Role of aldehyde dehydrogenases in endogenous and xenobiotic metabolism. Chem. Biol. Interact. **129:**1–19.
65. **Virtanen, T., and T. Kinnunen.** 2008. Clinical allergy and immunology series, p. 576. *In* R. F. Lockey and D. K. Ledford (ed.), Allergens and allergen immunotherapy, 4th ed. Informa Health Care, New York, NY.
66. **Wegrzyn, P., J. Jura, T. Kupiec, W. Piekoszewski, B. Wladyka, A. Zarebski, and A. Koj.** 2006. A search for genes modulated by interleukin-6 alone or with interleukin-1[beta] in HepG2 cells using differential display analysis. Biochim. Biophys. Acta **1762:**319–328.
67. **Wynn, T. A., R. W. Thompson, A. W. Cheever, and M. M. Mentink-Kane.** 2004. Immunopathogenesis of schistosomiasis. Immunol. Rev. **201:**156–167.
68. **Yamamoto, S., Y. Tomita, S. Nakamori, Y. Hoshida, H. Nagano, K. Dono, K. Umeshita, M. Sakon, M. Monden, and K. Aozasa.** 2003. Elevated expression of valosin-containing protein (p97) in hepatocellular carcinoma is correlated with increased incidence of tumor recurrence. J. Clin. Oncol. **21:**447–452.

Editor: J. F. Urban, Jr.